

THERMAL AND MECHANICAL LOADING OF THE ANODE GRID OF AN SHF GENERATOR WITH A VIRTUAL CATHODE OPERATING UNDER PULSED-PERIODIC CONDITIONS

A. E. Dubinov, V. D. Selemir,
V. A. Sidorova, N. I. Sel'chenkova, and
V. L. Sel'chenkov

UDC 621.385.6

We consider the increase in temperature and the resulting thermomechanical stresses in the anode grid of an SHF generator with a virtual cathode (vircator) under pulsed-periodic operating conditions.

In the past decade there has been appreciable progress in the creation of high-power nanosecond SHF-radiation generators with a virtual cathode on the basis of high-current relativistic electron beams (vircators) [1, 2]. Their merits, such as simple design and the possibility of operation without external magnetic tracking of the electron beam, determine their competitive ability among other classes of high-power relativistic superhigh-frequency devices.

Thus, the vircator developed in [3] has the following characteristics: the radiation power is 150 MW, the pulse duration is of the order of 20 nsec with a radiation wavelength of 3 cm. It was triggered pulsed-periodically with a pulse-repetition rate of 10 Hz [4] (see Fig. 1a).

A further increase in the pulse-repetition rate is desirable, but it encounters technical problems associated with the stability of the anode grid.

Below we carry out an analysis of the thermal and mechanical operating conditions of the anode grid for the above-indicated vircator with the following initial data: the diameter of the grid wires is 0.1 mm; the material of the wires is tungsten (the highest melting point is $T_{\text{melt}} = 3673$ K); the geometric transparency of the grid is 88%; the injected current in the vircator is 12 kA; the energy of the electrons is $eU = 100$ keV; the diameter of the beam of electrons near the anode grid is $d = 4$ cm.

The transverse structure of the beam together with the anode grid is shown in Fig. 1b, from which it is seen that the central wire is subjected to the greatest energy effect, which is a pulse current $I = 5$ A distributed over a length $\sim d$.

First we consider the thermal operating conditions of the grid, namely, ohmic heating of the wire and thermal shock [5], during which heat is lost mainly by thermal radiation (much as in [6]). In conformity with this, we write the temperature-balance equation in the form

$$c\rho \frac{\partial T}{\partial t} = \lambda \left(\frac{\partial^2 T}{\partial r^2} + \frac{1}{r} \frac{\partial T}{\partial r} \right) + I^2 R + IU - \varepsilon \sigma A (T^4 - T_0^4), \quad (1)$$

where $T = T(r, t)$ is the temperature distribution; T_0 is the initial temperature; A is the area of the side surface of the wire; ε is the emissivity of the wire surface; σ is the Stefan-Boltzmann constant. The physical constants of tungsten [7, 8] are mass density $\rho = 1.93 \cdot 10^4$ kg/m³, specific heat $c = 142$ J/(kg·K), and specific thermal conductivity $\lambda = 167$ W/(m·K). The temperature dependence of the emissivity given in [9] in the form of a table, was approximated by us in the following manner:

$$\varepsilon(T) = 0.042 + 0.000127(T - 500). \quad (2)$$

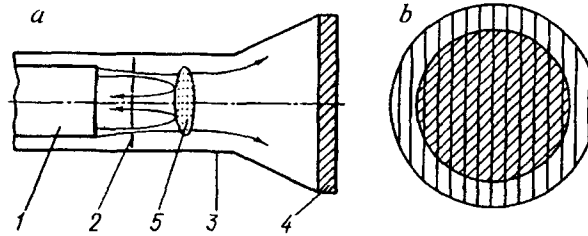


Fig. 1. Scheme of the vircator: a) vircator in section [1) cathode, 2) anode grid, 3) drift tube, 4) radiation outlet window, 5) virtual cathode], b) anode grid (the cross section of the beam is hatched).

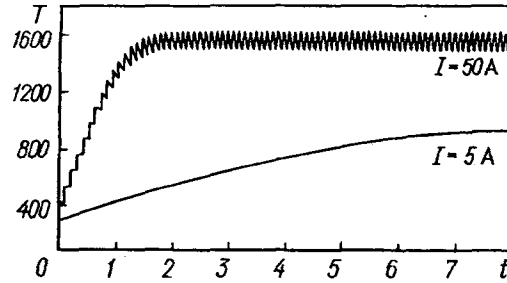


Fig. 2. Evolution of the anode grid temperature. T , K; t , sec.

A numerical comparison of the terms on the right-hand side of Eq. (1) shows that the ohmic heating is very small compared to the thermal shock and that the thermal conductivity can be neglected on nanosecond time scales. With these simplifications, Eq. (1) was solved numerically by the Runge–Kutta method. Typical time behavior of the wire temperature for a specified current $I = 5$ A and for a current exceeding it by an order of magnitude is illustrated in Fig. 2, from which it is seen that the average value of the temperature approaches saturation. Here, the temperature is far from the melting point with a considerable reserve.

This, however, should not mean that there are no problems with the stability of the anode grid at the specified level of the action (the current incident on the wire, the energy of the electrons, the pulse-repetition rate), since the shock-induced mechanical stresses can exceed the strength characteristics of the grid material.

In analyzing the mechanical stresses, we use a thermoelasticity equation for the displacements u :

$$\frac{\partial^2 u}{\partial r^2} + \frac{1}{r} \frac{\partial u}{\partial r} - \frac{u}{r^2} = \alpha \frac{1 + \mu}{1 - \mu} \frac{\partial T}{\partial r}, \quad (3)$$

where $\mu = 0.29$ is the Poisson coefficient; $\alpha = 4.4 \cdot 10^6$ is the coefficient of linear thermal expansion [7, 8]. Taking into account the fact that the range of electrons with an energy of 100 keV amounts to about 0.015 mm, we may assume that energy release occurs in a thin surface layer of the wire. In this case the radial and azimuthal stresses can be written, respectively, in the form [10]:

$$\sigma_{rr} = \frac{2G}{1 - 2\mu} \left[(1 - \mu) \frac{\partial u}{\partial r} + \mu \frac{u}{r} \right] - \frac{\alpha ET}{1 - 2\mu}; \quad (4)$$

$$\sigma_{\varphi\varphi} = \frac{2G}{1 - 2\mu} \left[(1 - \mu) \frac{u}{r} + \mu \frac{\partial u}{\partial r} \right] - \frac{\alpha ET}{1 - 2\mu}, \quad (5)$$

where $G = E/2(1 + \mu)$ is the shear modulus; $E = 4 \cdot 10^{11}$ N/m² is Young's modulus. Simultaneous solution of Eqs. (3) and (4), (5) yields

$$\sigma_{rr} = \frac{2\alpha ET}{(1 - \mu) r_0} \sum_{n=1}^{\infty} \frac{1}{\beta_n^2 J_1(\beta_n r_0)} \left[\frac{r_0}{r} J_1(\beta_n r) - J_1(\beta_n r_0) \right]; \quad (6)$$

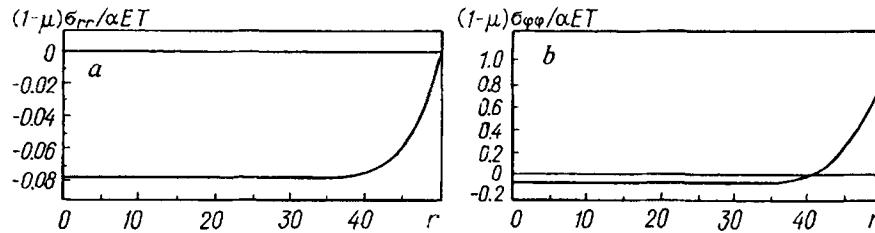


Fig. 3. Radial distribution of radial (a) and azimuthal (b) stresses. r , μm .

$$\sigma_{\varphi\varphi} = \frac{2\alpha ET}{(1-2\mu)r_0} \sum_{n=1}^{\infty} \frac{1}{\beta_n^2 J_1(\beta_n r_0)} \left[\beta_n r_0 J_0(\beta_n r) - J_1(\beta_n r_0) - \frac{r_0}{r} J_1(\beta_n r) \right], \quad (7)$$

where $J_0(\beta_n r_0) = 0$; r_0 is the wire radius. Typical distributions of the mechanical stresses σ_{rr} and $\sigma_{\varphi\varphi}$ over the radius of the wires are shown in Fig. 3. Numerical evaluations indicate that already at $T = 1000$ K these stresses exceed the static limit of strength of tungsten.

Thus, it is shown that under pulsed-periodic operating conditions an anode grid can be subjected to considerable mechanical loading, and this precludes the possibility of a further increase in the pulse-repetition rate and requires special measures for increasing their stability.

The authors wish to express their gratitude to V. V. Kulik for useful discussions of the results of the work.

REFERENCES

1. B. V. Alyokhin, A. E. Dubinov, V. D. Selemir, et al., IEEE Trans. Plasma Sci., 22, No. 5, 945-959 (1994).
2. A. E. Dubinov and V. D. Selemir, Zarubezh. Radioelektr., No. 4, 54-60 (1995).
3. B. V. Alekhin, V. V. Voronin, S. L. Voronov, et al., in: Abstracts of Papers of the 13th Kharkov Seminar on Linear Accelerators of Charged Particles [in Russian], Kharkov (1993), p. 24.
4. V. D. Selemir, B. V. Alekhin, A. E. Dubinov, et al., in: New Industrial Technologies, Issue 2 (268) [in Russian], 1995, pp. 53-55.
5. G. A. Mesyats and D. I. Proskurovskii, Pulsed Electrical Discharge in Vacuum [in Russian], Novosibirsk (1984).
6. J. Keizer, L. W. Maki, J. Greathouse, et al., J. Phys. Chem., 99, 844-852 (1995).
7. Yu. V. Koritskii, V. V. Pasyukov, and B. M. Tareev (eds.), Handbook of Electrical-Technology Materials [in Russian], Leningrad (1976).
8. I. S. Grigor'ev and E. Z. Meilikhov (eds.), Physical Quantities: Handbook [in Russian], Moscow (1991).
9. K. J. Smithells, Tungsten [Russian translation], Moscow (1958).
10. G. Parkus, Transient Temperature Stresses [Russian translation], Moscow (1963).